Available online at www.sciencedirect.com
ScienceDirect
Journal of the European Ceramic Society 29 (2009) 1933–1938
www.elsevier.com/locate/jeurceramsoc

Three-step sintering of constrained yttria stabilised zirconia layers and its effect on microstructure and gas permeance☆

Gary J. Wright [b,*,1], Julie A. Yeomans [a]

[a] *School of Engineering, University of Surrey, Guildford, Surrey, GU2 7XH, UK*
[b] *Rolls-Royce Fuel Cell Systems Limited, Loughborough, Leicestershire, LE11 3GR, UK*

Received 26 September 2008; received in revised form 6 December 2008; accepted 10 December 2008
Available online 20 January 2009

Abstract

Three-step sintering has been applied to constrained yttria (3 mol%) stabilised zirconia (YSZ) layers. The sintering schedules use a coarsening stage (step one) prior to reaching the peak temperature (step two). Once the peak temperature has been reached the temperature is lowered and an isothermal dwell takes place (step three). As the YSZ layers form part of a solid oxide fuel cell, and thus need to prevent the fuel and air from mixing, gas flow across the layers was measured and gas permeance values calculated. Several of the three-step sintering schedules produced layers with lower gas permeance values compared with a conventional sintering schedule that is used currently. Further, a three-step schedule produced one of the lowest gas flow rates and minimised the maximum temperature exposure thus offering several potential benefits in terms of processing options.

Keywords: Sintering; Grain size; ZrO_2; Fuel cells

1. Introduction

In the majority of solid oxide fuel cells (SOFCs), yttria stabilised zirconia (YSZ) is the ionically conducting electrolyte. As well as providing the conduction path, the electrolyte must keep the gas streams on either side of the fuel cell from mixing.[1,2] In the integrated planar design (IP-SOFC) the YSZ electrolyte is a thin layer, deposited via methods such as screen-printing, and once sintered it can be $\leq$10 μm in thickness.[3] In SOFCs there is a need to reduce the sintering temperature of the electrolyte to reduce the cost of fabrication and also limit the possibility of interactions between the electrolyte and the electrode materials.[4] The drive to reduce sintering temperature while maintaining a gas tight electrolyte is a challenge. The electrolyte needs to densify sufficiently so as to maintain the separation of the fuel and air gas streams but ideally the temperature should be lower than, or at the low end of, the range 1300–1550 °C, which is usually associated with the unconstrained sintering of YSZ.[5,6] In the IP-SOFC, the layer is constrained so the freedom of movement is restricted for the in-plane direction and therefore the ceramic body is only free to move normal to the substrate. This constraint has been shown to retard the sintering process and change the densification rate of YSZ,[7] thus increasing the processing challenges that need to be overcome.

When assessing relative density of the layer, it is important to also consider grain size. Although an increase in grain size for dense electrolytes operating at 800–1000 °C was shown to have no obvious effect on the conductivity of the layer,[8] there are other implications. Earlier work has shown that there is a need to keep the YSZ grain size to a fraction of the layer thickness.[9] If the ratio of the grain size to the layer thickness is denoted as z then $0.1 < z < 0.3$ has been found to correspond with the lowest values of gas permeance. Thus, for a layer thinner than 10 μm, the grain size must be kept around 1 μm.

Previous studies of this system have considered conventional[9] and two-step sintering.[10] In conventional sintering, the sample is heated to an elevated temperature, held at that temperature for several hours, then cooled. In the two-step sintering method, originally proposed by Chen and

☆ Supported by Rolls-Royce plc., UK.
* Corresponding author at: School of Engineering, University of Surrey, Guildford, Surrey, GU2 7XH, UK. Tel.: +44 1332 241243; fax: +44 1332 248248.
E-mail address: gary.wright@rolls-royce.com (G.J. Wright).
[1] Based in part on the thesis submitted by G.J. Wright for the degree of Doctor of Philosophy, University of Surrey, Guildford, UK, 2006.

0955-2219/$ – see front matter © 2008 Elsevier Ltd. All rights reserved.
doi:10.1016/j.jeurceramsoc.2008.12.013

Wang, the sample is heated to an elevated temperature (T_1) and then immediately cooled to a lower temperature (T_2) and held there for longer times than in conventional sintering.[11] Studies on free bodies made from nanoscale powders have shown that it is possible to achieve densification without significant grain growth using two-step sintering.[12–14] Conventional sintering of constrained YSZ layers (1 h dwell at 1450 °C) has been shown to produce a layer with a relative density of 0.91 (corresponding to a thickness of 9 ± 0.8 μm) with a grain size of 1.3 ± 0.8 μm.[9] In two-step sintering, with a T_1 of 1600 °C and a 10-h dwell at a T_2 of 1100 °C a relative density of 0.97 (corresponding to a thickness of 7.4 ± 0.4 μm) and a grain size of 9.6 ± 1.6 μm was achieved. This shows that almost full density could be achieved but that it was accompanied by a substantial increase in grain size. However, separating the two-step sintering cycle into its component parts also showed that heating the sample to temperature T_1 gave a high relative density (0.98) with a grain size of 8.8 ± 1.5 μm. Therefore, as achieving a high density was the goal of sintering, the second part of the two-step sintering cycle would appear to be redundant in this case.

However, while the grain size at T_1 was smaller than that measured at T_2, 8.8 μm compared with 9.6 μm, the pore structure changed during the second part of the two-step sintering cycle. Pore size decreased from 2.4 ± 1.4 μm to 1.4 ± 0.6 μm and the pore size range (smallest to largest) also reduced from 0.5–6.0 μm to 0.5–3.9 μm. These changes in the pore size suggest that the microstructure is continuing to evolve in the second part of the sintering cycle. Although the application of two-step sintering to a constrained YSZ layer was shown to have benefits, it was not possible to reach the gas permeance targets associated with commercial fuel cells.[10] Hence, there is still a need to optimise the sintering of the YSZ electrolyte.

In this study the first aim is to investigate the potential for achieving full density using a novel three-step sintering procedure, which includes a coarsening section at the beginning of the sintering cycle.[15–17] The second aim is to evaluate the influence of three-step sintering on the z value and to test the hypothesis that a value between 0.1 and 0.3 gives the lowest gas permeance.

2. Experimental procedure

2.1. Sample preparation

YSZ is a typical material used for the electrolyte in SOFCs and in most cases 8 mol% YSZ is used. However, in the IP-SOFC, 3 mol% YSZ powder is used and a commercially available powder (MEL Chemicals, Manchester, UK) was chosen for this study. YSZ powder was mixed with a terpineol based binder, 63/2 Medium (Johnson Matthey, Stoke-on-Trent, UK) to produce an ink that could be screen-printed. Ink was applied to a ~30-μm thick, pre-fired priming layer on a porous magnesia rich magnesium aluminate spinel substrate (Advanced Ceramics Limited, Stafford, UK) using a SMTECH Benchmark 90 screen-printer. The quantity of ink deposited on the surface of the substrate is defined by the screen mesh size. A mesh thickness of 110 ± 3 μm relates to a mesh size of 165 apertures/in. (API) and an area of 2500 mm^2 was covered with the YSZ ink.

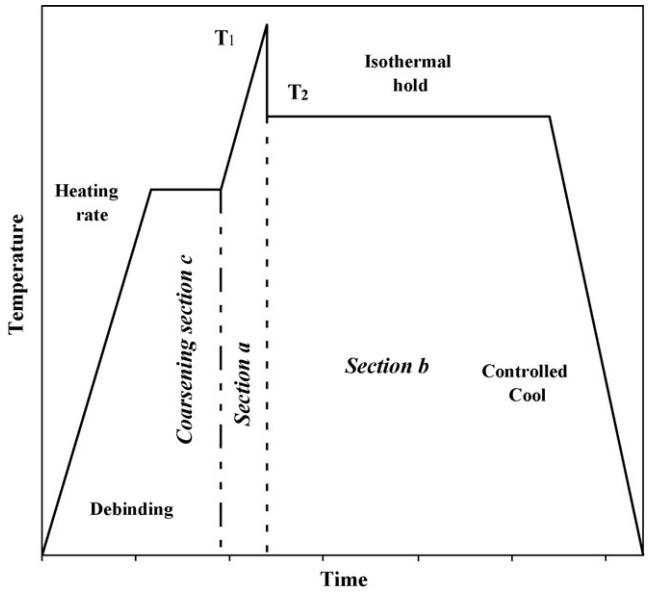

Fig. 1. Schematic illustration of a three-step sintering profile. The heating regime is shown as having three discrete sections: the coarsening (*section c*/step one), heating to T_1 (*section a*/step two) and isothermal hold at T_2 (*section b*/step three).

Three screen-printed layers were applied to the substrate with each layer being dried at 80 °C for 30 min in air prior to the next print application. Five samples were printed for each sintering cycle that was investigated.

The three-step sintering process is shown schematically in Fig. 1. A heating rate of 10 °C min^{-1} was applied throughout. The dwell before the maximum temperature is termed the coarsening stage (step one); the isothermal dwell was for 2 h at 1100 °C. Then the sample was heated to the maximum temperature, T_1 and held for 5 min; this corresponds to the first section, in two-step sintering (step two). Then the temperature was dropped to T_2 and held for 10 h (step three). Sintering cycles can be identified by the three temperatures associated with the isothermal dwells as shown in Table 1; other sintering cycles have been included for comparison.

2.2. Microstructural characterisation

The microstructure of the sintered layers was observed using a scanning electron microscope (SEM, Cambridge Stereoscan 240, Cambridge Instruments, Cambridge, UK). Grain and pore size measurements were taken using the linear intercept method, British Standard BS EN 623-3:2001. Relative density was calculated from the grain and pore size measurements to provide a value for the planar surface of the sintered layers. Samples were imaged in cross-section to measure the sintered layer thickness. Three measurements/sample were taken; one at each edge and one in the middle of the layer.

2.3. Gas permeance

The sintered YSZ electrolytes were tested using room temperature gas leakage apparatus. Gas permeance values are

Table 1
Details of samples processed using three-step sintering profiles (two-step values for comparison). The errors represent one standard deviation from the mean.

Sample no.	Peak temperature, T_1 (°C)	Temperature, T_2 (°C)	Sintered layer thickness (μm)	Relative density	Mean grain size (μm)	Mean pore size (μm)	Pore size range (μm)
1450-1[9]	1450	–	9.0 ± 0.8	0.91	1.3 ± 0.1	0.8 ± 0.3	0.3–2.3
1400-1200[17]	1400	1200	8.3 ± 0.6	0.90	1.4 ± 0.1	0.8 ± 0.2	0.2–2.4
1100-1400-1200	1400	1200	7.4 ± 0.4	0.82	0.9 ± 0.1	0.8 ± 0.3	0.1–3.3
1367-1300[19]	1367	1300	6.9 ± 0.4	0.87	0.7 ± 0.1	0.7 ± 0.3	0.2–1.7
1100-1367-1300	1367	1300	7.3 ± 0.5	0.89	0.8 ± 0.2	0.6 ± 0.2	0.2–1.7
1500-1300[18]	1500	1300	7.2 ± 0.8	0.92	2.8 ± 1.9	0.8 ± 0.4	0.2–2.9
1100-1500-1300	1500	1300	7.0 ± 0.6	0.94	5.1 ± 1.2	1.0 ± 0.2	0.4–2.4
1600-1150[17]	1600	1150	7.4 ± 0.4	0.97	9.6 ± 1.6	1.4 ± 0.6	0.5–3.9
1100-1600-1150	1600	1150	8.2 ± 0.3	0.98	8.6 ± 1.5	1.3 ± 0.9	0.5–2.5

calculated from the gas flow rate and differential pressure across the sintered layer.[9]

3. Results and discussion

3.1. Microstructural characterisation

In all cases samples attained a density of ∼0.9 theoretical density and above, corresponding to thicknesses between ∼7 μm and 9 μm. Cross-sections through the layers are shown in Fig. 2, while the relative densities, mean grain sizes, mean pore sizes and pore size ranges are shown in Table 1. In the majority of cases, the addition of the coarsening step offers no advantage e.g. 1100-1400-1200 has a significantly lower density than 1400-1200 and 1100-1500-1300 has a larger grain size than 1500-1300,[18] whereas 1100-1367-1300 is comparable with 1367-1300.[19] However, 1100-1600-1150 does offer advantages over 1600-1150 in that the densities are comparable (0.98 and 0.97) and although there was no significant change in the mean pore size, there was a reduction in the distribution from 0.5–3.9 μm to 0.5–2.5 μm, indicating that the coarsening section influences the pore structure.

3.2. Microstructural evolution during the coarsening stage

In order to understand the microstructural changes that were occurring during the coarsening section, samples were sintered at 1050 °C, 1100 °C and 1150 °C for 2 h. As the temperature increased the grain size also increased and mean pore size shows a significant increase between 1100 °C and 1150 °C, as shown

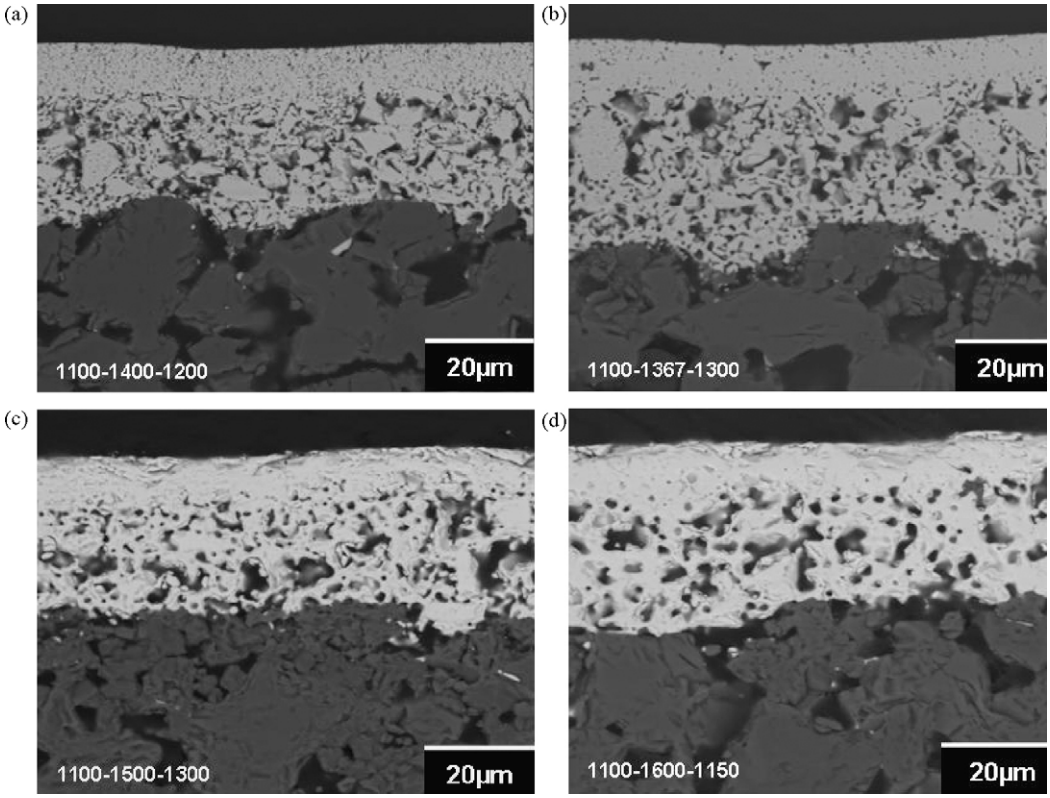

Fig. 2. Scanning electron micrographs of cross-sections of sintered layers sintered using three-step method (a) 1100-1400-1200, (b) 1100-1367-1300, (c) 1100-1500-1300 and (d) 1100-1600-1150.

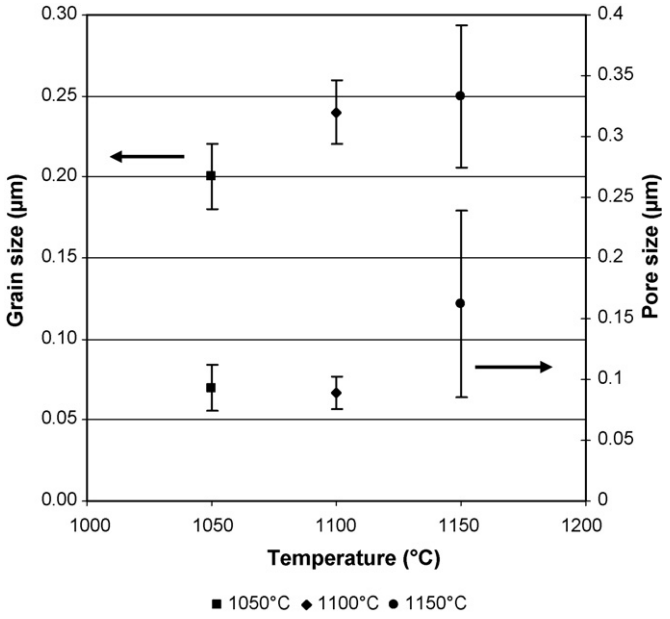

Fig. 3. Grain and pore size as a function of temperature for samples heated to 1050 °C, 1100 °C and 1150 °C. Error bars represent one standard deviation from the mean.

in Fig. 3. Further, at 1150 °C there is a significant increase in the size of the error bars for both grain and pore size. Sintering at 1100 °C results in a narrower pore distribution than for either of the other two samples. This small reduction in the mean pore diameter and a narrowing of the distribution suggests the microstructure is more homogeneous and the pore network has redistributed, thereby increasing the likelihood of obtaining a higher density YSZ body.[20]

3.3. Gas permeance of the layers

The rate of gas flow across a sintered thick-film layer is dependent on the microstructure. Gas flow across samples sintered using three-step sintering was measured and the gas permeance values were calculated accordingly.[9] These gas permeance values are shown in Fig. 4 where three-step samples are compared with conventional (one-step) sintering. As the pressure changes there is a change in gas permeance for each sample and this variation increases slightly with increasing gas permeance. It is envisaged that a typical gas pressure across an electrolyte would be 30 mbar.[9] The three-step schedules produced gas permeance values below that of conventional sintering in all but one case (1100-1400-1200). The highest gas permeance was measured for sample 1100-1400-1200 ($1.7 \times 10^{-4} \pm 1.0 \times 10^{-5}$ mbar l s^{-1} cm^{-2} at 30 mbar) while the lowest gas permeance values were for samples 1100-500-1300 ($6.8 \times 10^{-5} \pm 7.3 \times 10^{-6}$ mbar l s^{-1} cm^{-2} at 30 mbar) and 1100-1367-1300 ($7.0 \times 10^{-5} \pm 3.4 \times 10^{-6}$ mbar l s^{-1} cm^{-2}). The two-step equivalent of samples 1500-1300 and 1367-1300 showed slightly higher mean gas permeance ($7.7 \times 10^{-5} \pm 5.3 \times 10^{-6}$ mbar l s^{-1} cm^{-2} and $8.2 \times 10^{-5} \pm 2.0 \times 10^{-5}$ mbar l s^{-1} cm^{-2} at 30 mbar, respectively).

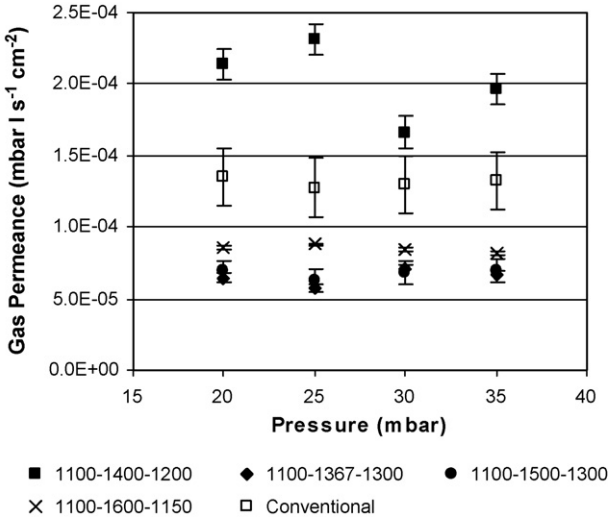

Fig. 4. Gas permeance as a function of pressure through thick-film layers sintered using three-step and conventional sintering profiles.

3.4. Relationship between microstructural parameters and gas permeance

Earlier work showed that a minimum gas permeance was associated with a z factor (ratio of grain size to layer thickness) of between 0.1 and 0.3 for conventionally sintered samples. Using two-step sintering the z factor range increases to 0.4 and becomes less sensitive to gas permeance. The three-step sintering schedules do not produce samples with z values within this range. The two lowest gas permeance values were measured for samples with z factors of 0.1 (1100-1367-1300) and 0.7 (1100-1500-1300), as shown in Fig. 5. It would appear that as the number of steps in the sintering process increases the gas permeance becomes less sensitive to the z factor alone and that other parameters become important when considering the flow of gas across the thick film.

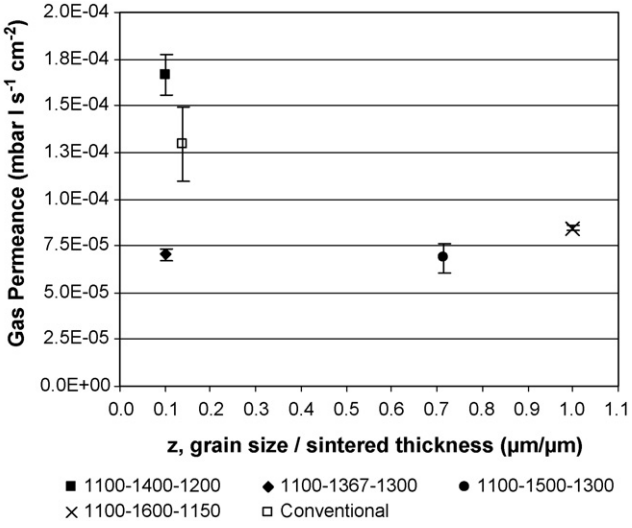

Fig. 5. Gas permeance at a pressure of 30 mbar as a function of the ratio of grain size to sintered layer thickness, z.

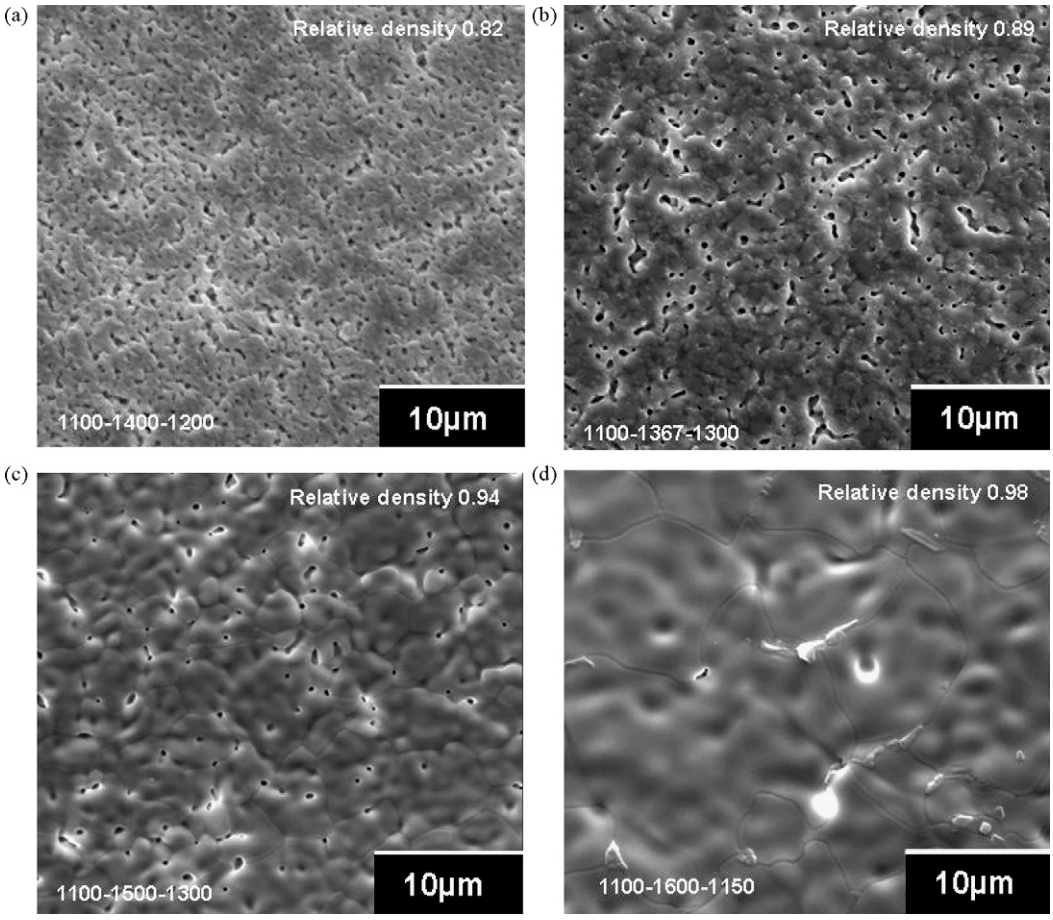

Fig. 6. Scanning electron surface micrographs of the three-step sintering samples (a) 1100-1400-1200, (b) 1100-1367-1300, (c) 1100-1500-1300 and (d) 1100-1600-1150.

Three-step sintering produces a range of surface microstructures, as shown in Fig. 6. Where there are samples with similar gas permeance values, 1100-1500-1300 has achieved a higher density (0.94 compared with 0.89) and has a significantly larger mean grain size (5.1 μm compared with 0.8 μm) than 1100-1367-1300. However, it should be noted that other samples have achieve a higher density (e.g. 1100-1600-1150) and thus gas permeance is not a simple function of density. For the two samples with low gas permeance values, the coarsening and dwell temperatures (T_2) are the same. The only difference in the sintering of these samples is the peak temperature (T_1), 1500 °C and 1367 °C. It would appear that the relatively short time spent at 1500 was significant in terms of densification and grain growth. Clearly, further work is needed to clarify the optimum density and grain size to achieve a gas permeance value that is acceptable for constrained YSZ thick-films intended for application as a fuel cell electrolyte.[10] However, since the three-step sintering schedules do produce samples that have lower gas permeance values than the sample sintered conventionally, and lower than the two-step equivalent in most cases, they merit further investigation.

An additional, indirect benefit from this type of sintering cycle comes from other limitations within the application. Given that the YSZ layer is constrained by adjacent layers that contain metallic components, sintering cycles which reduce the peak sintering temperature lead to a greater choice of metals and the avoidance of unwanted chemical reactions. Thus, from this perspective 1100-1367-1300 has advantages over both 1100-1500-1300 and the conventional sintering at 1450 °C.

4. Conclusions

The three-step sintering technique has been applied to constrained YSZ and compared with conventional (one-step) and two-step sintering. Three-step sintering introduces a coarsening section to the sintering profile prior to reaching the peak sintering temperature. It has been proposed that the inclusion of this initial step causes the microstructure to re-organise such that a treatment at 1100 °C creates a narrower pore size range. Sintering of constrained YSZ using this approach achieved relative densities of 0.89 and greater, but significant grain growth was observed. Whilst a high relative density could be achieved (0.98), this sample did not result in the lowest gas flow rate across the sintered layers. Although the density is an important parameter, other factors, such as the grain size, are important in minimising the gas permeance. One of the three-step sintering schedules where the temperature did not exceed 1367 °C, gives significant benefit both in terms of lower gas permeance and lower temperature processing compared with conventional sintering at 1450 °C.

Acknowledgements

The authors would like to acknowledge Dr Graeme Roberts (MCS, Roslin, Midlothian, UK) for performing the calibrating the SEM sufficiently to meet the ASTM standard and SEM analysis and Rolls-Royce Fuel Cell Systems Limited for their support with the gas testing.

References

1. Minh, N. Q., Ceramic fuel cells. *J. Am. Ceram. Soc.*, 1993, **76**(3), 558–563.
2. Bujalski, W., Paragreen, J., Reade, G., Pyke, S. and Kendall, K., Cycling studies of solid oxide fuel cells. *J. Power Sources*, 2006, **157**, 745–749.
3. Steele, B. C. H., Survey of materials selection for ceramic fuel cells: I. Electrolytes and bi-polar plates, ceramic oxygen ion conductors and their technological applications. *Proc. Br. Ceram. Soc.*, 1996, **56**, 151–162.
4. Delaforce, P. M., Yeomans, J. A., Filkin, N. C., Wright, G. J. and Thomson, R. C., Effect of NiO on the phase stability and microstructure of yttria-stabilized zirconia. *J. Am. Ceram. Soc.*, 2007, **90**(3), 918–924.
5. Young, W. S. and Cutler, I. V., Initial sintering with constant rates of heating. *J. Am. Ceram. Soc.*, 1970, **53**(12), 659–663.
6. Luo, J., Adak, S. and Stevens, R., Microstructure evolution and grain growth in the sintering of 3Y-TZP ceramics. *J. Mater. Sci.*, 1998, **33**, 5301–5309.
7. Bordia, R. K. and Scherer, G. W., On constrained sintering I. Constitutive model for a sintering body, II. Comparison of constitutive models, III. Rigid inclusions. *Acta Metall.*, 1988, **36**(9), 2393–2416.
8. Han, M., Tang, X., Yin, H. and Peng, S., Fabrication, microstructure and properties of a YSZ electrolyte for SOFCs. *J. Power Sources*, 2007, **165**, 757–763.
9. Wright, G. J. and Yeomans, J. A., The influence of screen-printing parameters on the microstructure and gas permeance of a zirconia electrolyte. *J. Eur. Ceram. Soc.*, 2008, **28**(4), 779–785.
10. Wright, G. J. and Yeomans, J. A., Constrained sintering of yttria stabilized zirconia electrolytes: the influence of two-step sintering profiles on microstructure and gas permeance. *Int. J. Appl. Ceram. Technol.*, 2008, **5**(6), 589–596.
11. Chen, I. W. and Wang, X. H., Sintering dense nanocrystalline ceramics without final-stage grain growth. *Nature*, 2000, **404**(March), 168–171.
12. Wang, X. H., Chen, P. L. and Chen, I. W., Two-step sintering of ceramics with constant grain-size, I: Y_2O_3. *J. Am. Ceram. Soc.*, 2006, **89**(2), 431–437.
13. Wang, X. H., Deng, X. Y., Bai, H. L., Zhou, H., Qu, W. G., Li, L. T. *et al.*, Two-step sintering of ceramics with constant grain-size, II: $BaTiO_3$ and Ni-Cu-Zn ferrite. *J. Am. Ceram. Soc.*, 2006, **89**(2), 438–443.
14. Binner, J., Ketharam, A., Paul, A., Santacruz, I. and Vaidhyanathana, B., Dense nanostructured zirconia by two stage conventional/hybrid microwave sintering. *J. Eur. Ceram. Soc.*, 2008, **28**(5), 779–785.
15. Wang, J. X., Wang, X. P., Liang, F. J., Cheng, Z. J. and Fang, Q. F., Enhancement of conductivity in $La_2Mo_2O_9$ ceramics fabricated by a novel three-stage thermal process method. *Solid State Ionics*, 2006, **177**, 1437–1442.
16. Bodhak, S., Basu, B., Venkateswaran, T., Jo, W., Jung, K. H. and Kim, D. Y., Mechanical and fretting wear behaviour of novel (W,Ti)C–Co cermets. *J. Am. Ceram. Soc.*, 2006, **89**(5), 1639–1651.
17. Wolff, M., Braun, A., Falk, G. and Clasen, R., Sintering conditions of translucent zirconia ceramics made of nanosized powders. In *Sintering 2003*, 2003.
18. Lee, S. Y., Sintering behaviour and mechanical properties of injection—molded zirconia powder. *Ceram. Int.*, 2004, **30**, 579–584.
19. Leite, E. R., Paskocimas, C. A., Longo, E., Barrado, C. M., Godinho, M. J. and Varela, eJ. A., Two steps sintering of yttria stabilized zirconia. In *Sintering 2003*, 2003.
20. Lin, F. J. T., De Jonghe, L. C. and Rahaman, M. N., Microstructure refinement of sintered alumina by a two-step sintering technique. *J. Am. Ceram. Soc.*, 1997, **80**(9), 2269–2277.